

Numerical analysis of eccentric orifice plate using ANSYS Fluent software

D Zahariea

Department of Fluid Mechanics, Fluid Machinery and Fluid Power Systems, Technical University
"Gheorghe Asachi" Iași, România

E-mail: dzahariea@yahoo.com

Abstract. In this paper the eccentric orifice plate is qualitative analysed as compared with the classical concentric orifice plate from the point of view of sedimentation tendency of solid particles in the fluid whose flow rate is measured. For this purpose, the numerical streamlines pattern will be compared for both orifice plates. The numerical analysis has been performed using ANSYS Fluent software. The methodology of CFD analysis is presented: creating the 3D solid model, fluid domain extraction, meshing, boundary condition, turbulence model, solving algorithm, convergence criterion, results and validation. Analysing the numerical streamlines, for the concentric orifice plate can be clearly observed two circumferential regions of separated flows, upstream and downstream of the orifice plate. The bottom part of these regions are the place where the solid particles could sediment. On the other hand, for the eccentric orifice plate, the streamlines pattern suggest that no sedimentation will occur because at the bottom area of the pipe there are no separated flows.

1. Introduction

One of the most important, common and long history of use methods for fluid flow measurement is the differential pressure device method (head-loss device method), for which the difference in pressure Δp measured at two points, upstream and downstream sides of the measurement device, is proportional with the rate of fluid flow.

The flow measurement device, which in this case, is a restriction device causing the obstruction to the fluid flow, will generate a pressure drop which will be measured with two pressure taps positioned upstream and downstream of the restriction device. The most common taps installed configurations are: flange pressure taps, corner pressure taps and vena contracta taps (D and $D/2$ pressure taps), [1]. There are many restriction devices such as nozzles, Venturi nozzles and Venturi tubes, but by far, the most commonly used restriction device for flow measurement in pipes is the orifice plate (orifice meter) which is designed usually as: squared-edged orifice plate, squared-edged with conical back-cut orifice plates, sharp-edged orifice plates, conical entrance orifice plates, quarter-circle entrance orifice plate, segmental orifice plate and eccentric orifice plates, [1].

In order to obtain the desired accuracy some requirements should be accomplished: the circularity of both the orifice and the pipe, the plate flatness, the roughness of the upstream plate surface, the sharpness of the orifice edge, the thickness of both the plate and the orifice, the pressure taps, the pipe roughness, the eccentricity (the distance between the pipe axis and the orifice axis). There are many results referring to orifice plates, from which, in this context, should be mentioned: the comparative numerical analysis of different orifice plates [2], the numerical analysis of orifice plate working under non-standard



conditions [3], as well as the comparative numerical analysis of single hole and multi hole orifice plates [4]. However, all this research is about the conventional concentric orifice plate. Despite the fact that for conventional orifice plates, the pipe and the orifice should be concentric, there are some exceptional circumstances for which the eccentricity should be an effective design option. The eccentric orifice plates are recommended for flow measurement of fluids with entrained gas, liquid or sediments for which the sedimentation of such inclusions can thus be avoided, [5].

The eccentricity of the orifice is defined by the difference between the pipe axis and the orifice axis, and for the particular case analyzed in this paper, can be expressed through the formula:

$$e = \frac{D}{2}(1 - \beta) \quad (1)$$

where D is the pipe diameter, $\beta=d/D$ is the diameter ratio, and d is the orifice diameter.

This paper discusses the numerical analysis of an eccentric orifice plate used for flow measurement of liquids using ANSYS Fluent software, as compared with the conventional concentric orifice meter. The eccentric orifice plate has the same orifice diameter as the concentric orifice plate.

2. Geometry

Both orifice meters are characterized by the same diameter ratio $\beta=d/D=0.5$, where $d=50$ mm is the orifice diameter and $D=100$ mm is the pipe diameter, as well as by the same pipe Reynolds number $Re=10^5$. Considering the fluid as water with density $\rho=998.2$ kg/m³ and dynamic viscosity $\mu=0.001003$ Pa·s, the fluid average velocity at the pipe inlet will result as $V=1.0048$ m/s and the mass flow rate will be $Q_m=7.8775$ kg/s. The eccentricity computed using the equation (1), is equal with 25 mm.

The orifice plate is located into a horizontal pipe with total length of $35D$, between two pipe sections, the upstream pipe section with length $L_1=15D$ and the downstream pipe section with $L_2=20D$, figure 1.

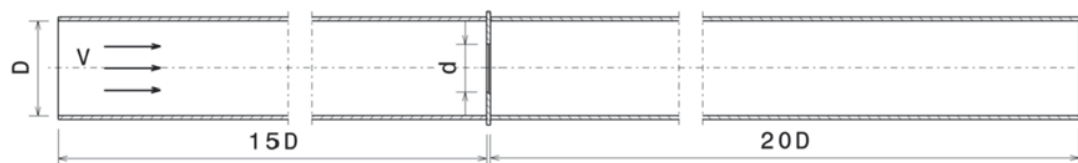


Figure 1. Geometry of the computational domain.

Because of the longitudinal symmetry of the geometry, a longitudinal symmetry cutting plane has been used, thus only one half of the pipe geometry will be modeled. The 3D model has been created using CATIA. The 3D geometric model has been transferred in ANSYS using the STP file format. The solid domain geometry of the orifice meters is presented in figure 2 for the concentric orifice plate, and in figure 3 for the eccentric orifice plate.

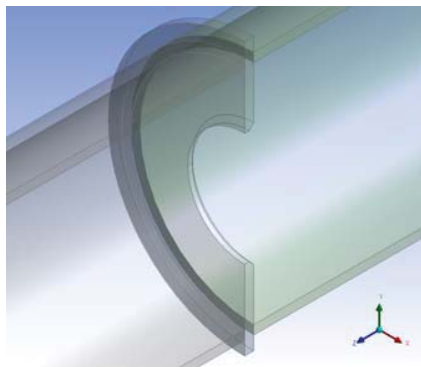


Figure 2. Concentric orifice plate-solid domain.

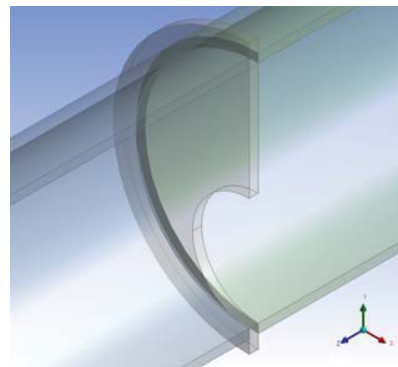


Figure 3. Eccentric orifice plate-solid domain.

3. Mesh

Using fluid flow domain extraction techniques, the fluid flow domain has been obtained. The fluid flow domains from the orifice plate zone are presented in figure 4 for the concentric orifice plate, and in figure 5 for the eccentric orifice plate.

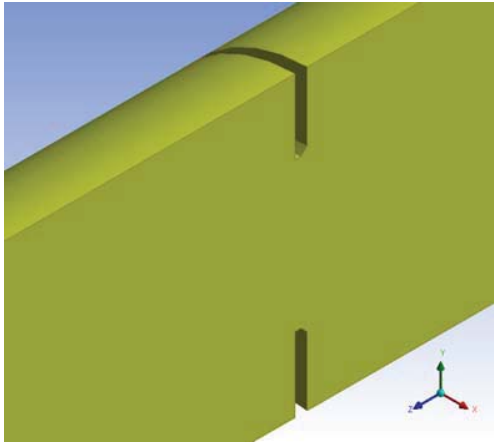


Figure 4. Concentric orifice plate-fluid domain.

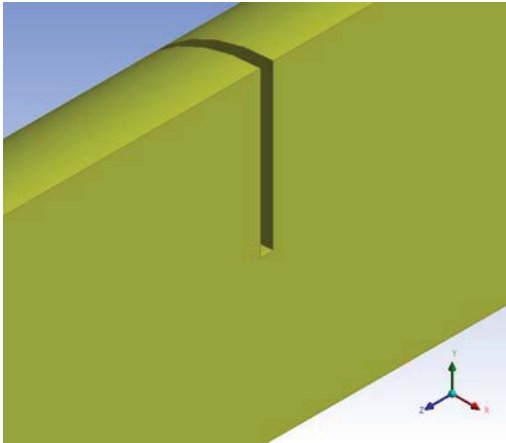
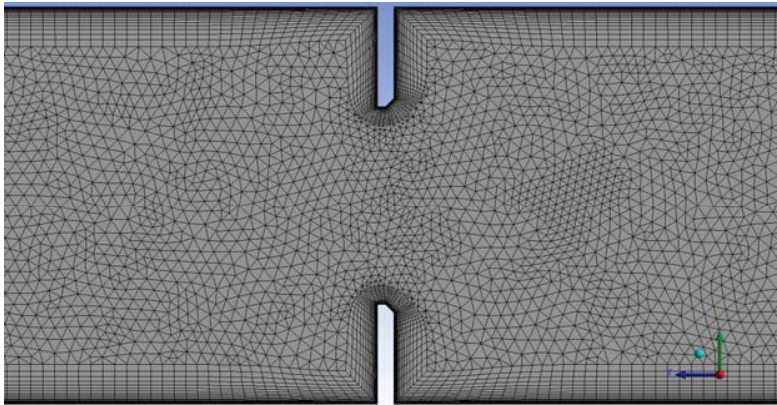
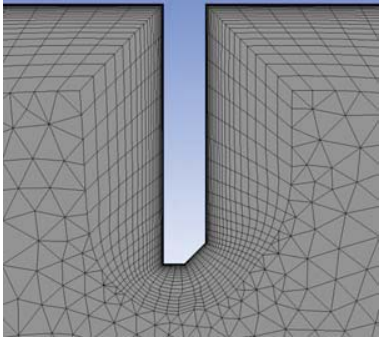


Figure 5. Eccentric orifice plate-fluid domain.

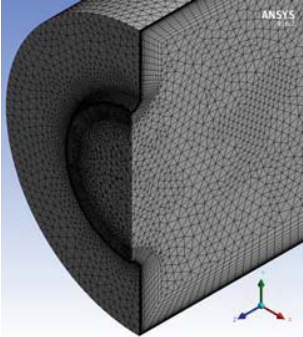
The mesh obtained for the concentric orifice plate is presented in figure 6.



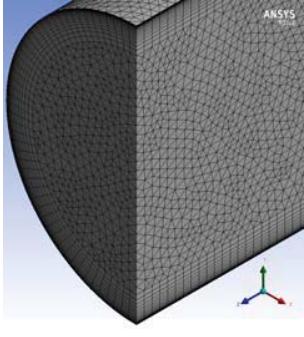
a) symmetry plane detail



b) concentric orifice plate detail



c) section plane detail



d) inlet section detail

Figure 6. Concentric orifice plate - mesh.

The mesh obtained for the eccentric orifice plate is presented in figure 7.

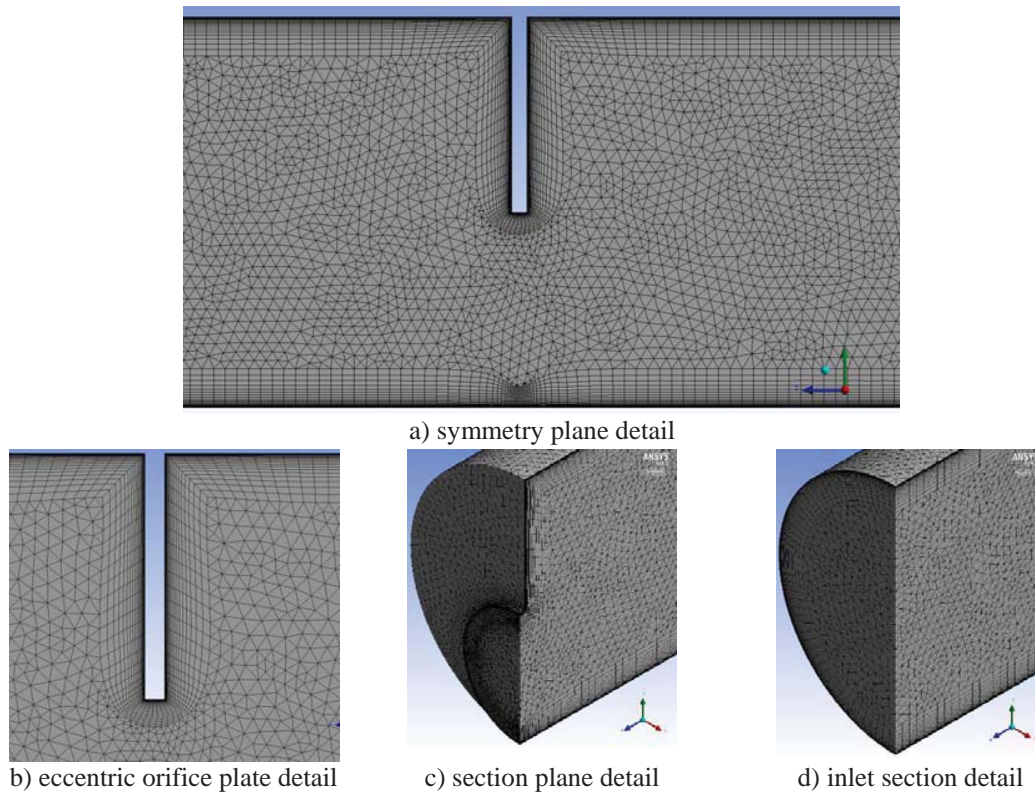


Figure 6. Eccentric orifice plate - mesh.

Both the mesh for concentric orifice plate, as well for the eccentric orifice plate has been obtained using Mesh application from ANSYS Workbench. In order to properly resolve the boundary layer along the fluid domain walls, as well as around the orifice plate an inflation mesh property has been defined with 25 layers and the first layer thickness adjusted for the dimensionless wall distance $y^+ \cong 1$. The mesh principal parameters are presented in table 1.

Table 1. Mesh characteristics.

Orifice plate	Nodes	Elements	Skewness
Concentric	2496422	6650615	0.896
Eccentric	2455446	6550947	0.916

4. CFD analysis

The CFD analysis has been performed using Fluent software for solving the Reynolds-Averaged Navier-Stokes equations with the following main settings: $k - \omega$ SST turbulence model; steady pressure based solver with SIMPLE pressure-velocity coupling algorithm with second order upwind spatial discretization for momentum, turbulent kinetic energy and specific dissipation rate.

The boundary conditions of the problem are: the velocity $V=1.0048$ m/s on the inlet section; the atmospheric pressure on the outlet section; no-slip boundary condition at the flow domain walls, as well as at the orifice plate walls; zero normal velocity and zero normal gradients of all variables at the symmetry plane; the effect of gravity has been considered.

The convergence criterion of the steady state solution obtained by the CFD analysis has been defined as a sum of three convergence check criteria: the residual error for continuity, for x-, y- and z-velocity, for turbulence kinetic energy k and for specific rate of dissipation ω should be under 10^{-4} ; the pressure at the inlet section, as one of the relevant variable of the analysis, should reach a steady solution; the relative mass flow rate imbalance between the inlet and the outlet sections should be less than 1% of the smallest mass flow through the flow domain. The convergence has been obtained after 880 iterations for concentric orifice plate analysis, and after 1283 iterations for the eccentric orifice plate analysis. At the convergence point, the relative mass flow rate imbalance is 3.12e-04% for concentric orifice plate and 5.82e-04% for the eccentric orifice plate.

The computations have been parallelized performed on 32 cores of a SUPERMICRO workstation with 4 Intel XEON E5-4640 2.4 GHz processors, 256 GB DDR4 RAM, 2 TB HDD and NVIDIA Quadro K4000 3 GB GDDR5 video card.

5. Results

The streamlines, both 3D and 2D, are presented in figure 7 for the concentric orifice plate, and in figure 8 for the eccentric orifice plate.

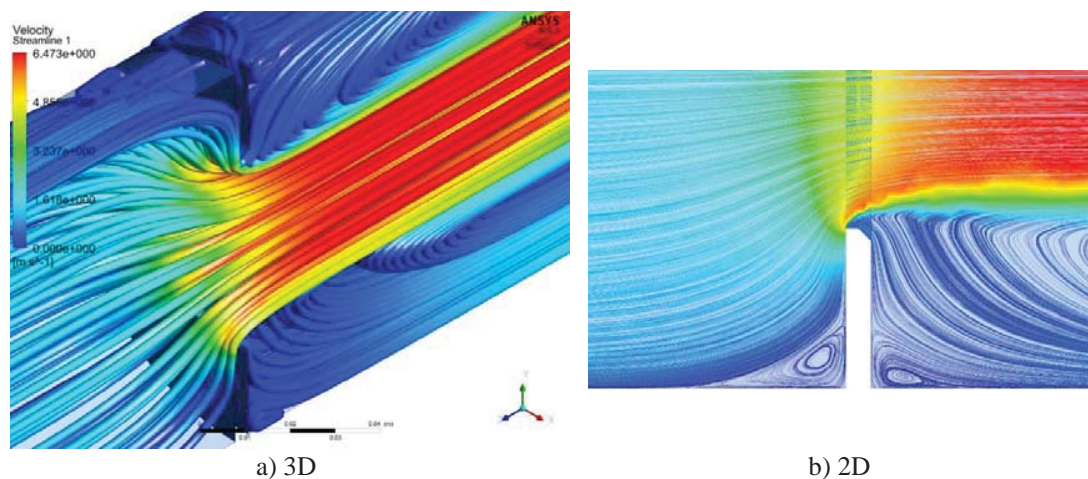


Figure 7. Concentric orifice plate - streamlines.

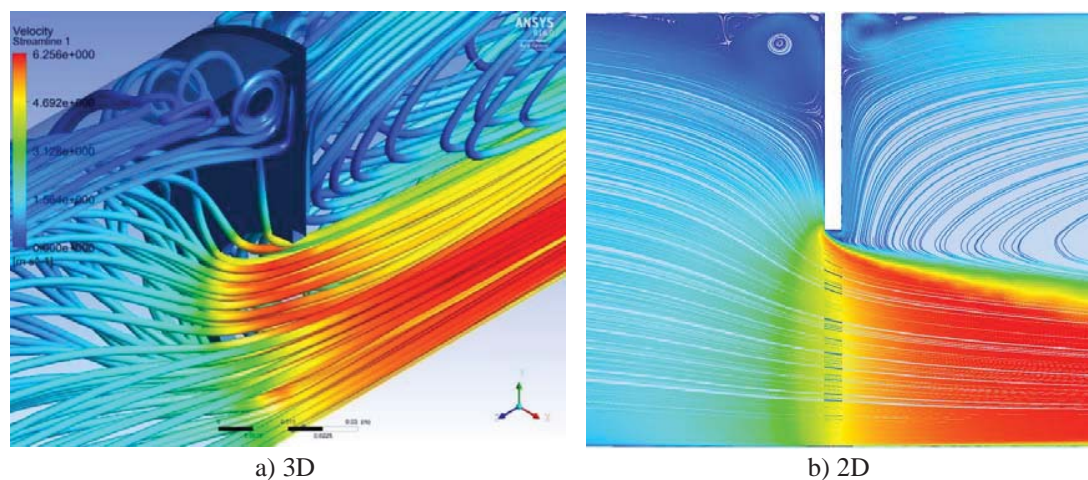


Figure 8. Eccentric orifice plate - streamlines.

6. Validation

The validation of the CFD analysis has been done by comparing the CFD results with the results provided by the standards ISO 5167, [1] and ISO TR 15377, [5] in terms of discharge coefficient.

The discharge coefficient is defined as, [1]:

$$C = \frac{4Q_m \sqrt{1 - \beta^4}}{\varepsilon \pi d^2 \sqrt{2\rho \Delta p}} \quad (2)$$

where $\varepsilon=1$ is the expansion factor.

The validation results are presented in table 2.

Table 2. Validation results.

Orifice plate	Pressure tappings	Discharge coefficient, C		Relative error
		Standard	CFD	
Concentric	D and D/2	0.6062	0.6084	0.36%
	Flange, ± 25.4 mm	0.6062	0.6117	0.90%
	Corner, ± 3 mm	0.6069	0.6707	10.50%
Eccentric	Corner, ± 3 mm	0.6270	0.6887	9.83%

7. Conclusions

The pressure drop across the orifice plate computed by CFD analysis is in very good agreement with the standard results, but starting from a certain distance from the orifice plate. In the close vicinity of the orifice plate, the errors are increased, and for this reason, further mesh improvement are required. However, the qualitative results obtained related with the streamlines pattern, confirm that the separated flow areas at the bottom part of the pipe, upstream and downstream of the concentric orifice plate where the solid particles could sediment, are not present for the eccentric orifice plate, and as consequence, for the eccentric orifice plate the sedimentation process will be avoided.

Acknowledgments

The author would like to acknowledge the computational resources offered by the Computer-Aided Fluid Engineering Laboratory from the Department of Fluid Mechanics, Fluid Machinery and Fluid Power Systems, Technical University “Gheorghe Asachi” Iași, Romania. The Computer-Aided Fluid Engineering Laboratory has been equipped with hardware and software resources with the financial support of the grant ENERED, POSCCE-A2-O2.2.1-2009-4, ID 911.

References

- [1] ISO 5167 2003 Measurement of fluid flow by means of pressure differential devices inserted in circular cross-section conduits running full
- [2] Sridevi T, Sekhar D and Subrahmanyam V 2014 Comparison of Flow Analysis Through a Different Geometry of Flowmeters using Fluent Software *Int. J. of Research in Eng. and Technol.* **3(8)** 141-149
- [3] Karthik G S, Kumar K J Y and Seshadri V 2015 Prediction of Performance Characteristics of Orifice Plate Assembly for Non-Standard Conditions Using CFD, *Int. J. of Eng. and Technical Research* **3(5)** 162-167
- [4] Malatesch B, Ganesha T and Math M C 2014 CFD Analysis and Comparison of Fluid Flow Through a Single Hole and Multi Hole Orifice Plate, *Int. J. of Research in Advent Technol.* **2(8)** 6-15
- [5] ISO/TR 15377 2007 Measurement of fluid flow by means of pressure-differential devices – Guidelines for specification of orifice plates, nozzles and Venturi tubes beyond the scope of ISO 5167